Scholars' Mine

Masters Theses   Student Theses and Dissertations

Fall 2007

Energy efficient processor operation and vibration based energy harvesting schemes for wireless sensor nodes

Phani Kumar Gajjala

ENERGY EFFICIENT PROCESSOR OPERATION AND VIBRATION

BASED ENERGY HARVESTING SCHEMES FOR WIRELESS

SENSOR NODES

by

PHANI KUMAR GAJJALA

A THESIS

Presented to the Faculty of the Graduate School of the

UNIVERSITY OF MISSOURI-ROLLA

In Partial Fulfillment of the Requirements for the Degree

MASTER OF SCIENCE IN COMPUTER ENGINEERING

2007

Approved by

_____   _____
Dr. Jagannathan Sarangapani   Dr. Sanjay Madria
Advisor

_____
Dr. Rosa Zheng

PUBLICATION THESIS OPTION

This thesis consists of the following two articles that have been submitted for publication as follows:

Pages 1-20 are intended for submission to the IEEE Transactions on Computer Aided Design of Integrated Circuits and Systems.

Pages 21-45 are intended for submission to IEEE Sensors Journal.

ABSTRACT

A Wireless Sensor Network (WSN) is a network of spatially distributed autonomous sensors deployed in the environment in order to cooperatively monitor physical or environmental conditions such as temperature, sound, pressure, motion or pollutants at different locations. Each node in a sensor network is equipped with a radio transceiver, a microprocessor and an energy source such as a battery which should be replaced periodically. To increase the lifetime of the network keeping the small size in mind, methods should be put in place to reduce the power consumption of the sensor node or increase the node life and/or to supply power to the battery from external sources.

In this thesis, the first paper presents an energy-efficient frequency adaptation based approach to minimize the power consumption of the microprocessor in an attempt to increase the lifetime of the sensor node. The proposed method dynamically changes the frequency at which the processor operates and puts it into sleep designated by a low frequency mode when no operation is performed. The simulation results show that proposed method consumes energy less compared to available methods.

The second paper, on the other hand, presents an energy harvesting circuitry to charge the battery of the sensor node so that the time to replacement can be extended. A piezoelectric-based energy harvesting circuitry and an equivalent mathematical model is proposed. The piezoelectric circuitry converts mechanical vibrations into electrical energy which is utilized to charge the battery. The simulation results using the mathematical model show that the circuitry harvests around 22.8mW of power which appears to be more than the power obtained from commercial harvesting devices.

ACKNOWLEDGMENTS

TABLE OF CONTENTS

LIST OF ILLUSTRATIONS

LIST OF TABLES

INTRODUCTION

The lifetime of the sensor node and the wireless sensor network is limited due to short battery life. Periodic replacement of battery is tedious and costly. Therefore in this thesis, the first paper presents a novel energy efficient frequency adaptation based approach to minimize the power consumption of the microprocessor in an attempt to increase the lifetime of the sensor node. The second paper presents an energy harvesting circuitry to charge the battery in the sensor node so that the time to replacement can be extended. A piezoelectric-based energy harvesting circuitry and an equivalent mathematical model is proposed. Simulation results show that the proposed method of minimizing the processor power consumption and energy harvesting can significantly extend the lifetime of the node and the network.

PAPER I

FREQUENCY ADAPTATION BASED APPROACH FOR MINIMIZIMING POWER CONSUMPTION IN A PROCESSOR

Phani Kumar Gajjala
University of Missouri - Rolla
Electrical and Computer Engineering Department
1870 Miner Circle
Rolla, Missouri 65409
USA

Maciej Zawodniok and Jagannathan Sarangapani
University of Missouri - Rolla
NSF I/UCRC Center for Intelligent Maintenance Systems
Electrical and Computer Engineering Department
1870 Miner Circle
Rolla, Missouri 65409

ABSTRACT

Power aware computing has become popular and many techniques have been proposed to manage processor energy consumption for real time applications. The main focus of this paper is to minimize the power consumption of the processor on the sensor node using frequency adaptation. Power consumption and task completion are often contradictory goals and power and time have to be judiciously managed to achieve the goal of minimizing energy. Processor consumes energy even in its idle state and operates at the same frequency at present. By contrast, in the proposed approach, the processor will operate in different power modes which are defined by a low frequency mode during idle periods and high frequency mode for task execution. By operating the processor at the low frequency mode, the processor minimizes the power consumption whereas the processor operates in the high frequency mode in order to meet the deadline constraints. Even in the high performance mode depending on the number of tasks queued in the input buffer, the clock frequency is altered dynamically by using dynamic programming. The proposed approach reduces power consumption of the processor and increases the lifetime of the sensor node.

1. INTRODUCTION

Battery powered portable systems have been widely used in many applications and there is a growing need for energy efficient designs that will enable higher performance devices with increased battery autonomy. Thus, extending battery life is one of the main research goals with these battery powered portable devices. Since battery technology has not kept pace with the increasing power demands of portable systems it is important to target power minimization during the design stage. It is known that power consumption is

proportional to frequency of operation. A significant challenge is to reduce the energy consumption during the operation of a certain task without extending its computation time. Figure 1 below shows the processor throughput as a function of time.
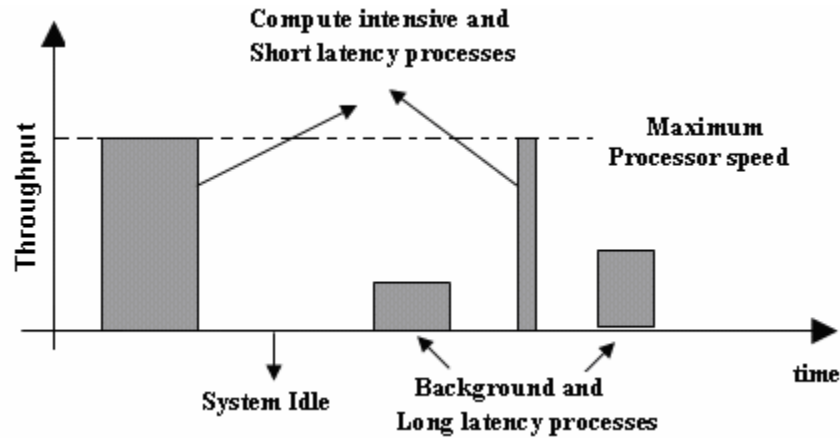
Figure 1. Processor usage model

The computational requirements of a task can be considered as computationally intensive, low speed or idle. Computationally intensive and short latency tasks utilize the full throughput of the processor. Low speed and high latency tasks only require a fraction of the full processor throughput to adequately run. There are system idle periods where the processor does not perform any tasks but consumes power. The key design objective for the processor systems in these applications is to provide the possible peak throughput for the computationally intensive tasks while maximizing the battery life for the remaining low speed and idle periods.

Broadly speaking there are two kinds of methods to reduce power consumption of processors. The first method aims at bringing the processor into a power down mode where only certain parts of the processor such as the clock generator and timer circuits are kept running when the processor is in idle state. Power modes are expected to have trade off between the amount of power saved and the latency incurred due to state

changes. Therefore for an real-time application where latency cannot be tolerated the applicability of power down may be restricted.

Another method is to dynamically change the speed of a processor by varying the clock frequency along with the supply voltage when the required performance on the processor is lower than the maximum performance. Slowdown using frequency scaling is known to be more effective approach but scaling the frequency of a processor leads to energy gains at the cost of increased execution time for a job or task. In real time systems energy consumption needs to be minimized while meeting the task deadlines. Power reduction and meeting timelines typically contradict and power and time have to be managed to achieve the goal. The frequency of the processor is altered dynamically according to the task by changing the frequency.

The paper is organized as follows. Section 2 presents the literature on the previous work done in this field. Section 3 presents motivations for this work. Section 4 explains the frequency adaptation based approach for minimizing power consumption of the processor. Section 5 presents and discusses the simulation results. Section 6 draws conclusions of the paper.

2. LITERATURE SURVEY

Since batteries continue to power an increasing number of electronic systems, their life becomes a primary design consideration. Figure 2 illustrates a widening battery gap between trends in processor power consumption [1] and improvements in battery capacity [2]. Bridging this gap is a challenge that system designers must face for the foreseeable future.
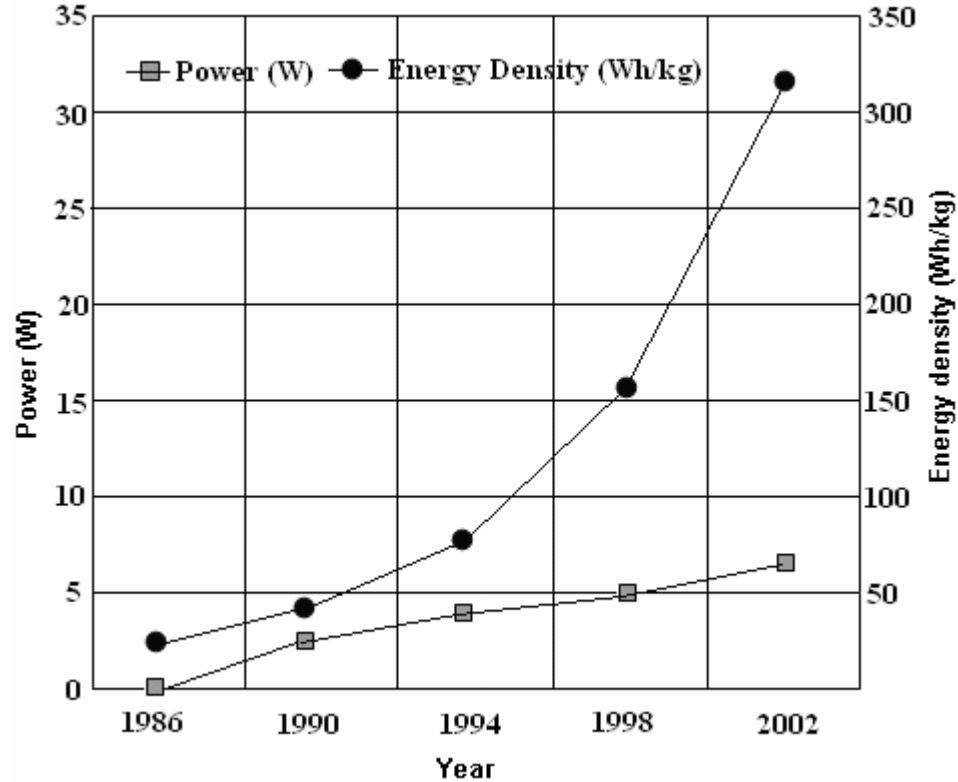
Figure 2. A widening battery gap between trends in processor power consumption.

Many system level power optimization techniques have been presented in the literature. The representative work includes voltage scaling [3, 4, 5], which refers to varying the speed of the processor by changing the clock frequency, supply voltage and power management. Here power management refers to the use of power down modes when a processor or a device is idle in order to reduce power consumption [6, 7]. Instead of focusing on reducing power consumption alone, researchers have started investigating the battery behavior and the effect of the battery discharge pattern on the battery capacity [8, 9, 10, and 11]. The work in [9, 10] suggests that reducing the discharge current level and shaping its distribution are essential for reducing the battery capacity loss.

On the other hand, a novel scheduling method to reduce power consumption by adjusting the clock speed together with supply voltage of the processor was first proposed in [12]

and was later extended in [13]. The basic idea includes the short term prediction of processor usage from the history of its utilization. From the predicted value, the speed of the processor is set to an appropriate value. However, due to latency during prediction, these methods cannot be applied to real time systems.

The scheduling algorithm in [14] was able to vary the voltage of the PEs (processing elements) that are voltage scalable in order to reduce the power consumption and manage the power profile of the entire system so that an improved battery efficiency results. The need to improve battery life is in large part has driven the research and development of low power design techniques for electronic circuits and systems [15, 16, 17, and 18]. Low power design techniques were successful in reducing the energy drawn from the battery and improving battery life. By understanding both the source of energy and the system that consumes it, the battery life can be maximized.

Frequency scaling techniques [19-20] use information from a battery model to vary the clock frequency of system components dynamically at run time. In particular, in [9], central processor unit (CPU) frequency scaling for battery powered systems is implemented. By contrast, a commonly used history based policy for CPU frequency scaling was presented in [19]. This policy dynamically calculates the CPU frequency for the next time interval based on run and idle time ratio values from the previous interval and amount of work left over. On the other hand, battery aware static scheduling algorithms aim at improving the system current discharge profile [20].

In [21], low power fixed priority scheduling (LPFPS) algorithm was proposed to reduce the power consumption of the processor. The algorithm uses two queues for active tasks- run queue holds the tasks that are waiting to run and delay queue holds the tasks waiting

for the next period. The processor executes the tasks in the order of priority. When the current task is completed and if there is a delay for the next task to arrive then the processor goes to a power down mode where it runs at a very low speed.

3. MOTIVATION

Power consumption has become one of the biggest challenges in high performance microprocessor design. Thus, reducing energy consumption and extending battery life have become a critical aspect of designing battery powered systems. Consider the four tasks given below in Table 1 where a) period determines the time when the task is executed again; b) time for execution determines the time the processor takes to complete the task when it operates at its highest frequency; and c) priority determines which task is to be executed first. Assume all the tasks are released simultaneously at the time zero.

Table 1. An example task set

Tasks	Periods (PT_i)	Priority (P_i)	Time for Execution (T_i)
1	50	1	10
2	80	2	5
3	100	3	10
4	120	4	10

The task 1 gets executed first as it has the highest priority followed by tasks 2, 3 and 4. A typical schedule assumes that the processor is running at the highest frequency as shown in Figure 3.
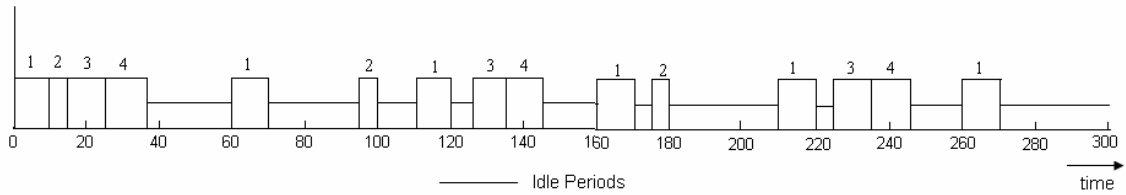
Figure 3. Schedule for the task set

There are many idle time intervals in the run time of the processor as shown in the figure above. At the time instant 60, when the request for the task 1 arrives, the processor knows that there will be no requests for any tasks until time instant 100 which is the time when the request for task 2 arrives. However, the processor still runs at highest clock frequency and stays idle for the rest of the time. The processor in its idle period consumes significant amount of energy since it operates at high clock frequency. The same is the case at time instants 40, 145, 180, 270. The amount of energy consumed by the processor in its idle period is given by Figure 4.
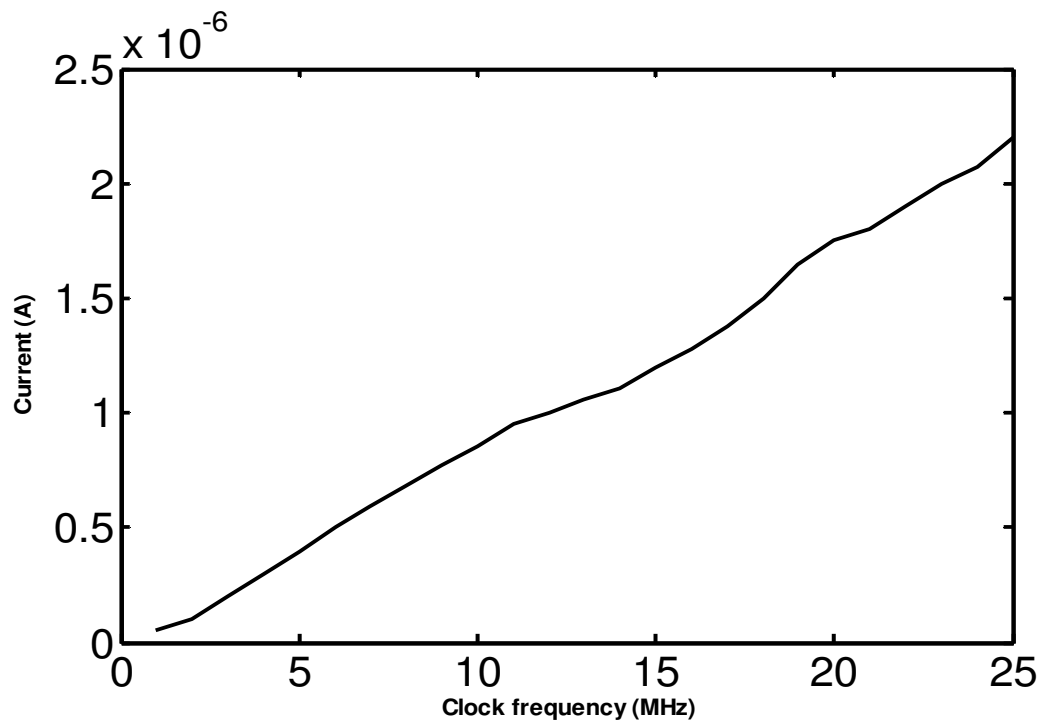
Figure 4. Current consumed in idle mode of the processor

From this figure, it is clear that the processor dissipates a lot of power in its idle state due to its significant current usage. Therefore, the main motivation is to minimize the unnecessary power consumption by running the processor at its lowest speed during its idle mode and to reduce the operating clock frequency when there are no tasks waiting in the queue. By adapting these two techniques, power can be saved. This approach is explained in the following section.

4. PROPOSED METHODOLOGY

The proposed frequency adaptation scheme minimizes energy consumption of the processor while maintaining the required level of service. The proposed mathematical model calculates and updates the clock frequency based on the tasks queued and the energy it has spent to complete the previous task. When there are no tasks to be executed in the queue the processor switches to the power down mode. First we determine the cost function for the queue occupancy and the energy spent for the execution of the task.

4.1 Buffer Occupancy State Equation

Consider the queue utilization equation given by

$$q_i(k+1) = q_i(k) + u_i(k) + w_i(k)$$

(1)

where $k = 0, 1, 2, \ldots\ldots, N-1$ is the time instant with N being the last step of the algorithm, $q_i(k)$ is the queue utilization at the time instant k in terms of number of instructions, $w_i(k)$ is the incoming traffic in terms of number of instructions at time instant k and $u_i(k)$ is the outgoing traffic in the form of number of instructions. The number of instructions can be translated into the processor clock frequency at the *time instant k*. The proposed scheme adjusts the clock frequency to minimize the energy

consumed by the processor since data sheets of processors indicate that higher the clock frequency higher is the energy consumption whereas the tasks are executed faster.

4.2 Queue Occupancy Cost

Consider a known ideal queue utilization q_{ideal} which renders the desired performance in terms of delay and throughput. The buffer cost can be written as a quadratic function of the error between ideal and actual queue utilization as

$$B(q_i(k)) = \gamma(q_i(k) - q_{ideal})^2 \tag{2}$$

where γ is the scaling factor and $q_i(k)$ is the current queue utilization. For instance, the cost of queue utilization is lowest when $q_i(k) = q_{ideal}$ and increases when the utilization is lower or higher than the desired value. To get a quadratic cost function, the queue utilization is substituted by the state variable

$$x_i(k) = q_i(k) - q_{ideal} \tag{3}$$

and cost function can now is expressed as

$$B(x_i(k)) = \gamma(x_i(k))^2 \tag{4}$$

The parameter γ will influence the convergence rate of the queue utilization to the target value. The higher the γ parameter the higher will be the cost spent on converging to the target queue utilization and corresponding performance level. The energy spent for the successful task execution depends upon the clock frequency obtained from $u_i(k)$.

4.3 Approximating Cost Function

The overall cost function for the rate adaptation scheme is expressed as

$$J_k(x_i(k)) = B(x_i(k)) + R_k(u_i(k))^2 + J_{k+1}(x_i(k+1)) \tag{5}$$

where $J_k(x_i(k))$ is the cost function from time instant k to N with initial state $x_i(k)$, $B(x_i(k))$ is the cost of queuing, $R_k(u_i(k))^2$ is the energy spent by the processor for the execution of a task which depends on the clock frequency of the processor $u_i(k)$ and $J_{k+1}(x_i(k+1))$ is the approximated cost for $K+1$ which is the next step. The final cost equation is expressed as

$$J_k(x_i(k)) = Q_k(x_i(k))^2 + R(u_i(k))^2 + J_{k+1}(x_i(k+1)) \tag{6}$$

where $Q_k = \gamma$ and $R_k = P_0(k)$ is the power consumed for a particular task. The cost function in (6) is in a quadratic form so we calculate an optimal feedback control law using the Riccatti equation (Bertsekas 1987) due to the linear nature of buffer dynamics provided the queue does not saturate. First we notice that the frequency adaptation problem should match closely the state of the system x_i to the outgoing flow w_i rather than the queue utilization since keeping an adequate flow of data is more important than keeping the queue at a certain level. Hence, a new state variable is considered which is equal to the sum of state x_i and outgoing flow w_i (negative value)

$$z_i(k) = x_i(k) + w_i(k) \tag{7}$$

Now substituting the new state (2) in (6) yields

$$J_k(z_i(k)) = Q_k(z_i(k))^2 + R_k(u_i(k))^2 + J_{k+1}(z_i(k+1)) \tag{8}$$

Applying the dynamic programming approach to (3) yields

$$J_N(z(N)) = Q_N(z(N))^2 \tag{9}$$

$$J_k(z(k)) = \min_{u_k} E\{Q_k(z_i(k))^2 + R_k(u_i(k))^2 + J_{k+1}(z_i(k) + u_i(k))\} \tag{10}$$

First we expand (10) before the last iteration

$$J_{N-1} = \min_{u_{N-1}} E\{Q_{N-1}(z_i(N-1)^2 + R_{N-1}(u_i(N-1))^2 + Q_N(z_i(N-1) + u_i(N-1))^2\}$$
$$= Q_{N-1}(z_i(N-1)) +^2 \min_{u_{N-1}} E\{R_{N-1}(u_i(N-1))^2 + Q_N(z_i(N-1))^2 + Q_N z_i(N-1)u_i(N-1) + Q_N(u_i(N-1))^2\}$$

$$(11)$$

The minimization of (11) with respect to $u_i(N-1)$ is done by differentiating (11) and

equating it to zero, which yields

$$u^*(N-1) = -z_i(N-1).Q_N/(Q_N + R_{N-1}) \qquad (12)$$

By substituting $u_i(N-1)$ in (11) with (12) we get

$$J_{N-1}(z(N-1) = Q_{N-1}(z_i(N-1))^2 (\frac{-Q_N}{[Q_N + R_{N-1}]})^2 + Q_N(z_i(N-1))^2(1 - \frac{Q_N}{[Q_N + R_{N-1}]})^2 \qquad (13)$$
$$= G_{N-1}(z_i(N-1))^2$$

where

$$G_{N-1} = Q_{N-1} + \frac{Q_N(R_{N-1}^2 - R_{N-1}Q_N)}{(R_{N-1} + Q_N)^2}$$
$$= Q_{N-1} + Q_N[\frac{1 - Q_N}{(Q_N - R_{N-1})}] \qquad (14)$$

Following the above calculations we can obtain an optimal input for $k = N-2, N-3,.....0$.

Thus, an optimal law for every k is equal to

$$u_i^*(k) = \frac{-z_i(k)G_{N+1}}{(G_{k+1} + R_k)} \qquad (15)$$

where

$$G_n = Q_N$$
$$G_k = G_{k+1}[1 - (G_{k+1}/(G_{k+1} + R_k))] + Q_k \qquad (16)$$

Because the execution time for each task is unknown it is desirable to calculate a steady

state solution assuming an infinite flow of tasks or instructions. In such case (15)

becomes

$$u_k^*(k) = \frac{-z_i(k)G}{(G+R_k)} \tag{17}$$

where G is the stable state solution and $R_k = P_0(k)$ is a parameter of cost function with $P_0(k)$ being the energy consumed by the processor to execute the task. By Substituting (2) in (17) in we can calculate the feedback control law which directly depends upon the queue utilization and the clock frequency which is given by

$$u_k^*(k) = \frac{-G(z_i(k))}{(G+R_k)} \tag{18}$$

This control law is applied at every instant the processor executes a task in order to obtain the optimal clock frequency u^*. The variable u^* depends on $z_i(k)$ and $z_i(k)$ depends on the number of tasks queued in the input buffer and the previous queue utilization. By assuming that the number of instructions is directly proposal to the clock frequency, the variable u^* can be viewed as the number of instructions that have to be executed by the processor in order to both keep the queue utilization at the desired level and to minimize the power consumption of the processor.

5. SIMULATION RESULTS

The proposed frequency adaptation scheme dynamically alters the clock frequency of the processor and switches it into low frequency sleep mode when it is not executing any tasks. In order to evaluate the proposed method a number of examples were simulated and compared with the method where processor does not vary the frequency dynamically while executing the tasks. Here we assume that each job is represented in the form of number of instructions. The different cases considered for the simulation are given below.

Case 1: delay_queue = 1e*6 [10 0 20 0 30 0 40 0 50 0 0]

priority = [9 8 7 6 5 11 10 12 13 2 3]

Case 2: delay_queue = 1e*6 [10 0 0 30 40 50 0]

priority = [9 8 7 12 13 14 4]

Case 3: delay_queue = 1e*6 [30 25 30 0 0 0 0 10 25 0 35 0 0 45 25 40]

priority = [9 8 7 12 13 14 15 9 8 7 2 13 14 5 18 19]

Case 4: delay_queue = 1e*6 [20 30 10 0 0 0 0 0 50 0 0 0 25 35 45 0 0 0 0 0 50 0 0]

priority = [9 6 5 7 8 2 3 4 9 8 7 2 4 5 6 1 2 3 10 11 18 12 1 2]

The delay_queue term represents the jobs arriving into the queue every second and it also defines the number of tasks queued at any instant of time. Tasks are represented as number of instructions as shown in delay_queue. For example the first task in Case 3 has 30 million instructions in it and 0 represents that there no tasks at that time instant. Priority tells the processor which task should be executed first when there are multiple jobs queued. The current consumed by the processor when operating at different frequencies is obtained from the silicon laboratories [22] using which the power consumption can be calculated.

Simulations were carried out based on the four cases shown above. Figure 5 shows that the current usage by the processor for the two different protocols for the 4 cases considered. From Figure 5 it is clear that frequency adaptation protocol consumes less current usage than the constant frequency protocol which translates into less energy consumption. For the cases considered, Case 4 takes longer time as it had many tasks arriving at the input buffer so the power consumption is higher. By contrast, Case 2 consumes less power as the tasks arriving into the queue were fewer. Here the frequency

is calculated based on number of instructions in the buffer and the energy consumed is obtained from the processor data sheet based on the current usage.
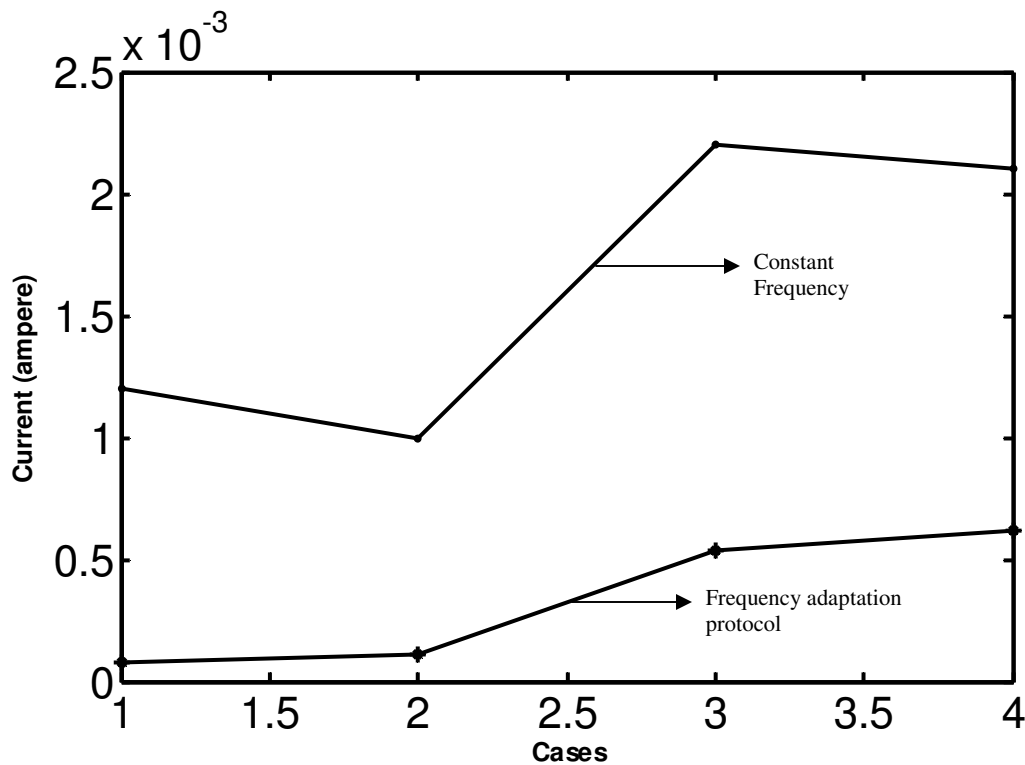
Figure 5. Comparison of protocols in terms of current usage.

From Figure 5, it can be observed that the frequency adaptation protocol consumes less current intake than the protocol which runs at constant frequency because the frequency adaptation dynamically varies the frequency based on the number of tasks (number of instructions) queued up. Energy consumed is directly proportional to the square of the current intake by the processor. If the number of tasks in the queue is fewer, the frequency is accordingly reduced to minimize current intake and energy consumption. On the other hand, if the tasks in the queue are higher the frequency is increased such that the jobs are finished sooner in order to meet the deadline. When the queue is empty, the processor goes into a sleep mode where it operates at a lower clock frequency which directly translates into low energy consumption. In the constant frequency case, the

processor operates at the same frequency irrespective of the number of tasks queued resulting in higher energy consumption.

In the next simulation, Case 4 is considered to study closely how the frequency adaptation protocol dynamically varies the frequency. Initially the clock frequency is set to 10Mhz for both the protocols. In Figures 6 and 7, the current usage for both the protocols for Case 4 is shown. From Figure 6, it can be observed that the processor operates only at two different frequencies- 10Mhz when it is executing a task and 5khz when it is in idle state. Because of executing all the tasks using high clock frequency of 10Mhz, the constant frequency protocol consumes significantly more current intake and energy.
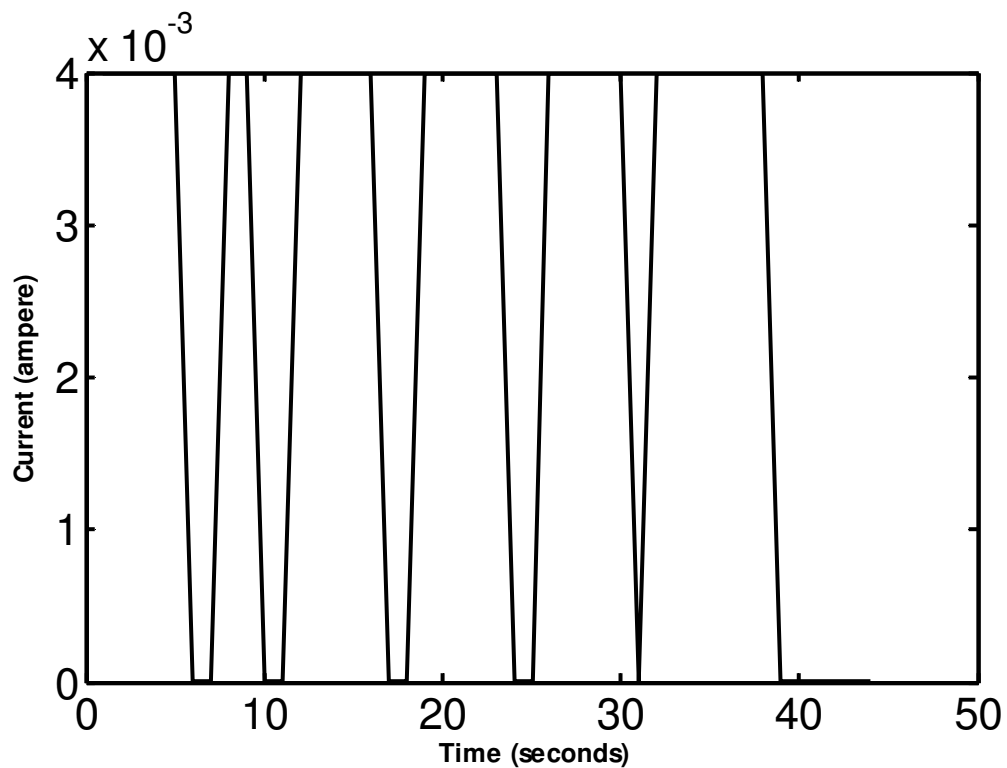
Figure 6. Current usage for the constant frequency protocol

Figure 7 depicts the power consumption of the frequency adaptation protocol for the Case 4. The frequency is dynamically varied due to the current usage varying with time. When the processor starts operating the queue has only the first task with 20 million instructions. At the next time instant, the task containing 30 million instructions arrives into the queue. Consequently, the proposed scheme increases the clock frequency using (18) in order to meet the deadline. Because of an increase in the frequency, current usage and power consumption increases. Additionally, it can be noticed that from 7 to 11 seconds, the processor switches into sleep mode due to successful completion of previous tasks and absence of any new tasks in the queue. The two peaks occurring at 22 and 27 seconds are due to more number of tasks stored in the queue at these times.
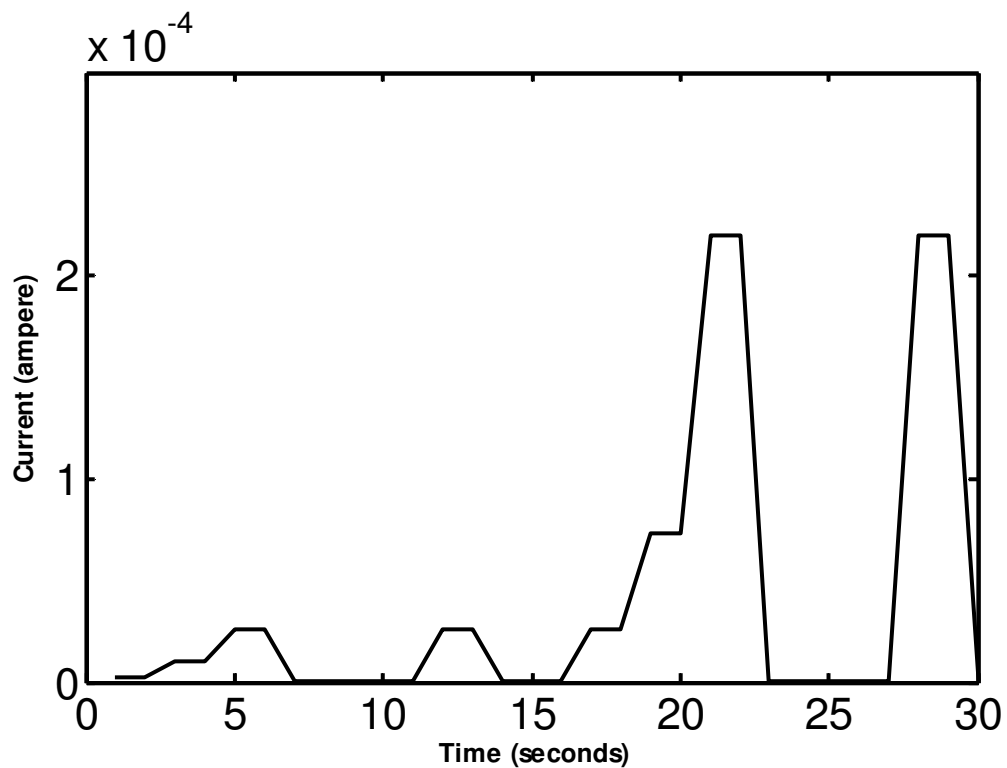
Figure 7. Current usage for the rate adaptation protocol.

6. CONCLUSIONS

In this paper, the problem of task scheduling in real-time for battery operated systems is addressed. An energy efficient frequency adaptation protocol using dynamic programming is presented for microprocessors. The proposed method renders reduced energy consumption for a processor by dynamically varying its clock frequency based on the number of tasks in the queue and switches the processor to a low frequency sleep mode when it is not executing any tasks. The proposed solution, which is simple and amenable to implementation, is shown to be safe and accurate enough to be used in a broad range of processors used in real world applications.

REFERENCES

[1] S. H. Gunther, F. Binns, D. M. Carmean and J. C. Hall, "Managing the Impact of Increasing Microprocessor Power Consumption," Intel Technology Journal, First Quarter, 2001.

[2] I. Buchmann, "Batteries in a portable world." http://www.cadex.com.

[3] I. Hong, D. Kirovski, M. Potkonjak and M. B. Srivastava, "Power optimization of variable voltage core based systems," IEEE Transaction Computer Aided Design, vol. 18, no 12, pp. 1702-1714, December 1999.

[4] Y. Shin and K. Choi, "Power conscious fixed priority scheduling for hard real time systems," Proceedings of the Design Automation Conference, pp. 134-139, June 1999.

[5] J. Luo and N. K. Jha, "Power conscious joint scheduling of periodic task Graphs and aperiodic tasks in distributed real time embedded systems," Proceedings of the Int Conf of Computer Aided Design, pp 357-364, November 2000.

[6] Q. Qiu and M. Pedram, "Dynamic power management based in Continuous time Markov decision process," Proceedings of the Design Automation Conference, pp. 555-561, June 1999.

[7] E. Y. Chung, L. Benini and G. De Micheli, "Dynamic power management using adaptive learning tree," Proceedings of the Int Conf on Computer Aided Design, pp. 274-279, November 1999.

[8] C. F. Chiasserini and R. R. Rao, "Pulse battery discharge in communication devices," Proceedings of the MOBICOM, pp. 88-95, August 1999.

[9] T. Martin, "Balancing batteries, power and performance: System issues in CPU speed setting for mobile computing," PhD dissertation, Carnegie Mellon University, Department of Electrical and Computer Engineering, August 1999.

[10] M. Pedram and Q. Wu, "Design consideration for battery powered electronics," Proceedings of the Design Automation Conference, pp. 861-866, June 1999.

[11] T. Simunic, L. Benini, and G. De Micheli, "Energy Efficient design of battery powered embedded systems," Proceedings of the International Symposium of Low Power Electronics and Design, pp. 212-217, August 1999.

[12] M. Wieser, B. Welch, A. Denners, and S. Shenker, "Scheduling for reduced CPU energy," Proceedings of the USENIX Symposium on Operating System Design and Implementation, pp 13-23, 1994.

[13] K. Govil, E. Chan, and H. Wasserman, "Comparing algorithms for Dynamic speed setting of a low power CPU," Proceedings of the ACM International Conference on Mobile Computing and Networking, pp 13-25, Nov 1995.

[14] Jiong Luo and Niraj K. Jha, "Battery Aware Static Scheduling for Distributed Real time Embedded Systems," DAC 2001, June 18-22, 2001.

[15] A. R. Chandrakasan and R. W. Brodersen, "Low Power Digital CMOS Design," Kluwer Academic Publishers, Norwell, MA, 1995.

[16] J. Rabaey and M. Pedram (editors), "Low Power Design Methodologies," Kluwer Academic Publishers, Norwell, MA, 1996.

[17] A. Raghunathan, N. K. Jha, and S. Dey, "High level Power Analysis and Optimization," Kluwer Publications, Norwell, MA, 1998.

[18] l. Benini and G. De Micheli, "Dynamic Power Management: Design Techniques and CAD Tools," Kluwer Publications, Norwell, MA, 1998.

[19] W. Weiser, B. Welch, A. Denners and S. Shenker, "Scheduling for reduced CPU energy," Proceedings of the USENIX Symposium Operating Systems Design, pp. 13-23, November 1994.

[20] J. Luo and N. K. Jha, "Battery aware static scheduling for distributed real time systems," Proceedings of the Design Automation Conference, pp.444-449, June 2001.

[21] Youngsoo Shin and Kiyoung Choi, "Power Conscious Fixed Priority Scheduling for Hard Real Time Systems" Proceedings of the ACM International Conference on Mobile Computing and Networking, pp 65-70, August 1999.

[22] Silicon Laboratories, "Power Management Techniques for the F30x and F31x". December 2006.

PAPER II

VIBRATION BASED ENERGY HARVESTING FOR WIRELESS

SENSOR NETWORKS

Phani Kumar Gajjala
University of Missouri - Rolla
Electrical and Computer Engineering Department
1870 Miner Circle
Rolla, Missouri 65409
USA

Shahab Mehraeen
Jagannathan Sarangapani
University of Missouri - Rolla
NSF I/UCRC Center for Intelligent Maintenance Systems
Electrical and Computer Engineering Department
1870 Miner Circle
Rolla, Missouri 65409

ABSTRACT

There is an increase in demand for wireless sensors and portable electronic devices due to remote sensing and smart embedded prognostic applications. As wireless devices are becoming ubiquitous, batteries are used to power these embedded devices. However, batteries are not durable and have to be replaced periodically. This procedure is costly especially for remote sensors or monitoring remote structures. Possible examples of such applications include health monitoring of earthmoving equipment and bridges since continuous data gathering is essential. Therefore, for many prognostic applications, it is of paramount importance to replace batteries with a more durable source of energy. One of the most applicable ways to solve this problem is to harvest energy from the environment. Energy harvesting is defined as the conversion of ambient energy into usable electrical form. Therefore, this paper details with the design of a novel piezoelectric generator to power the batteries. The piezoelectric generator is placed on a vibrating surface to convert the vibrations into electrical energy. A new piezoelectric generator design using the tapered beam is shown to harvest energy five times more when compared with a basic piezo generator using the standard rectangular beam.

2. INTRODUCTION

Wireless sensor networks (WSN) are composed of a set of autonomous microprocessor-based systems (nodes or motes) scattered in the ambient environment. Each node monitors physical quantities of the environment. Main applications of these sensor networks include the monitoring of environmental quantities such as temperature, sound, pressure, motion or pollutants at different locations. At present most of the sensor networks are composed of macro sized nodes (~10cm^2) made with standard ICs [1] and

non rechargeable batteries that lead to a finite lifetime. Research in sensors is targeted mainly on the low power consumption so that minimal maintenance is required. In order to satisfy the specification in terms of power and life time, energy harvesting is required. Sources of energy are necessary in order to perform functions like sensing, monitoring and communication. In these scenarios, energy is either stored internally or sent from a distance. The advantage of using the energy present in the immediate environment is to minimize or eliminate the need for internal sources of energy or the need to transport this energy from another location. Energy harvesting is not new to the mankind. For example light panels convert energy to power calculators. Solar planes are used in remote roads to power emergency cellular telephones eliminating the need to wire them externally.

Rotating machines such as generators, motors and combustion engines have efficiencies ranging from 20%-99% [2, 3]. In everyday experience, they waste considerable energy in the form of heat, sound and vibration. Often the wasted energy is large enough to power modern low power processors [4]. Thus harvesting the waste energy could provide enough power to perform useful low energy functions. A self powered sensor with wireless communication would greatly minimize the complexity and cost of monitoring and control, while enhancing reliability and flexibility.

Even if a sensor uses a battery, harvesting energy can decrease the energy demand on the battery and prolong its lifetime. The energy if present in excess at a particular moment can even be used to recharge the battery. There are various methods of energy harvesting and the most effective of those is the piezoelectric-based energy harvesting. Piezoelectric (PE) materials when mechanically loaded induce an electric charge on its opposite faces. Thus vibrating, compressing or flexing a PE material generates electricity. Over the past,

PE materials have been used in actuators, transducers and resonators. The magnitude and frequency of the vibration required to develop sufficient power, to drive the sensors are the main concerns for the development of the PE devices.

The paper is organized as follows. Section 2 presents the literature survey on the previous work done in this field of energy harvesting using vibration. Section 3 presents an overview of piezoelectric energy harvesting method to provide power to the battery of the sensor node. Section 4 presents and discusses the simulation results and Section 5 draws the conclusions of the paper.

2. LITERATURE SURVEY

Many researchers have investigated the problems associated with energy harvesting. Tores [5] suggested that extending battery life is particularly advantageous in systems with limited accessibility, such as biomedical implants and structure-embedded micro sensors. It was eluded that MEMS generators can act as self renewing sources, scavenging energy from different types of energy available in the environment. Since energy in the environment is not regulated in continuous form and will be available only in bursts, batteries such as thin film lithium-ion are still needed to store energy and deliver to the loading circuitry. Piezoelectric based ambient energy generator was modeled in [6] and experimentally validated for powering remote and long term sensing networks. Prior research has been done on vibration or vibration based power generators using electromagnetic [7, 8], electrostatic [9, 10] and piezoelectric [11, 12] conversion. Solar power is a promising alternative power source but it is not abundantly available for indoor applications.

2.1 Energy Harvesting Methods

There are several ways energy can be harvested from the environment and they should be compared by the power density, rather than energy density [5]. Energy can be harvested through vibration, which is based on the movement of a spring-mass vibrator. Vibration-based energy harvesting method consists of electromagnetic, piezoelectric, and electrostatic [1, 13]. Thermal energy is the second method of gathering energy from the environment and it is essentially based on temperature difference between opposite segments of a conducting material due to heat flow which can be used to produce a flow of charges. Finally energy from sunlight can be scavenged using photovoltaic cells [5]. To observe which form of energy harvesting is appropriate, Raghunathan *et al* [14] compared different energy harvesting methods as shown in the Table 1.

Table 1. Energy harvesting methods productivity

Harvesting Technology	Power Density
Solar Cells (outdoors at noon)	$15mW/cm^2$
Piezoelectric (PZT)	$330\mu W/cm^3$
Small Microwave Oven	$116\mu W/cm^3$
Electrostatic	$50-100\mu W/cm^3$
Thermoelectric (100C Gradient)	$40\mu W/cm^3$
Electromagnetic	$1\mu W/cm^3$
Acoustic noise (100dB)	$0.96\mu W/cm^3$

Although work in [14] focused on solar energy harvesting, useful information about storage devices used in energy harvesting is described since batteries are required in order to provide continuous source of energy to the devices. It was mentioned that batteries are relatively mature and have a higher energy density (more capacity for a given volume/weight) than ultra capacitors. However, ultra capacitors have a higher power density than batteries and are more efficient and therefore they offer higher lifetime in terms of charge-discharge cycles despite leakage issues. Commonly used rechargeable batteries include: Nickel Cadmium (NiCd), Nickel Metal Hydride (NiMH), Lithium based (Li+1), and Sealed Lead Acid (SLA). A comparison of the available batteries is briefly introduced. It was noted that SLA and NiCD batteries are not used as much because the former has a relatively low energy density, and the latter suffers from temporary capacity loss caused by shallow discharge cycles, termed as the memory effect.

One of the important issues in battery aging is the charge-discharge cycles. For example, NiMH batteries (when subjected to repeat 100% discharge) result in a lifetime of about 500 cycles, at which point the battery will deliver around 80% of its rated capacity. Environmental factors play a role in the design considerations. For example, battery self-discharge rate approximately doubles with every 10 degree increase in ambient temperature. Since the harvested power is extremely limited, considerations may apply to the design of power conversion circuitry. Also, the choice of battery chemistry for a harvesting system depends upon its power usage, recharging current, and the specific operating point on the cost-efficiency trade-off curve that a designer chooses.

2.2 Applications to Sensor Networks

Researchers have mainly focused on powering sensors with RF devices referred to as motes through energy harvesting. A standard assumption is made that the mote power consumption is extremely low which appears to be not realistic. Arms *et al.* [15, 16] have introduced a wireless sensor node consisting of embedded microcontroller, memory, sensor, radio transceivers using IEEE 802.15.4- 2.4 GHz, and a thin-film battery. A sleep/wake-up mode for the radio transceiver was utilized such that when the node wakes up from sleep, rapid synchronization to the network is achieved. This allows for low supply current, since radio may be rapidly switched on/off. It was noted that the power consumed by these wireless sensing nodes, when streaming data over the air continually, is around 45milliwatts. This consumption is reduced, to 5 milliwatts, by processing and/or logging data, rather than streaming it over the air. Power consumption of the mote is summarized in Table 2.

Table 2. Mote consumptions in different update rates

Update rate	1st gen. with radio (μW)	1st gen. w/o radio (μW)	2nd gen. w/o radio (μW)
0.1 Hz	25	20	50
1.0 Hz	100	50	55
5.0 Hz	420	150	70
10 Hz	825	300	90

A piezoelectric (PZT) micro generator consisting of a tapered flexure element with PZT mounted on the top and bottom of a cantilever beam (as shown in Figure 1) resonating at

the frequency of 60Hz is utilized. At the frequency of 57Hz, 2.7 milliwatts of power was obtained from the piezoelectric micro generator.
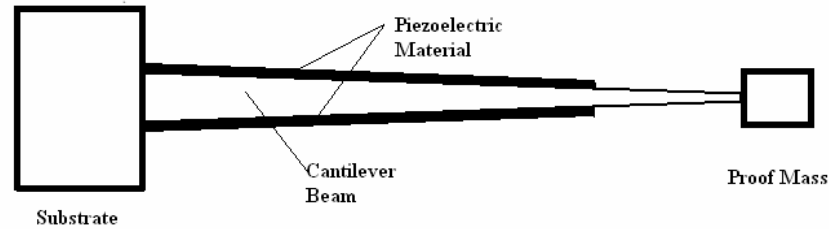

Figure 1. Cantilever beam

On the other hand, Clark *et al.* [17] and Ericka *et al.* [18] conducted analytical and experimental studies on circular unimorph piezoelectric plates. In [4], the feasibility of using piezoelectric materials as a power supply for an in vivo MEMS application was investigated. The micro generator was designed to drive a MEMS bio application consisting of an RF tag, which in turn needed 10mW. The device was expected to get energy harvested from human body. The mechanical to electrical conversion efficiency of PZT ceramic was assumed to be in the order of 34%. Thus a 10mW PZT-5A power supply will require 29.4mW which was shown to be available from human body. But as far as the generator size is concerned it was shown that the 10mW target could not be met. The researchers [4] proposed that current piezoelectric energy harvesting research falls into two key areas: developing optimal energy harvesting structures and highly efficient electrical circuits to store the generated charge or present it to the load circuit.

2.3 Mechanical Structure

Roundy *et al.* [5, 6, and 7] have built small cantilever-based devices using piezoelectric materials that can scavenge power from low-level ambient vibration sources. The beams were designed to resonate as close as possible to the frequency of the driving surface on

which they're mounted. The sensor node consists of a $1cm^3$ generator prototype to power a 1.9 gigahertz radio transmitter. The beacon has been powered at a duty cycle of 1 percent, which results in an average power consumption of 120 microwatts. The researchers in [6] have mainly focused on finding an efficient mechanical structure to transfer maximum possible strain to PZT. One design is based on building a piezoelectric generator on a two-layer bender (or *bimorph*) mounted as a cantilever beam. The device's top and bottom layers are composed of piezoelectric material. Roundy *et al.* [6] have indicated that by carefully choosing the relative layer thickness, the central layer improves overall electromechanical coupling.

A mathematical relationship for harvested power vs. frequency, mass, and PZT coupling coefficient has been provided in [6]. Roundy *et al.* [6] have recommend that a novel geometrical design should try to address at least one (if not all) of the following goals: (a)- maximize the piezoelectric response for a given input which can be accomplished either by maximizing the material's average strain for a given input or by changing the design to use direct coupling rather than the transverse coupling that piezoelectric bimorphs use; (b)- improve scavenger robustness by reducing stress concentration; (c)- minimize the losses (damping) associated with the mechanical structure.

It was found that power output drops dramatically as the vibrating frequency deviates from the natural frequency of the structure. It was demonstrated that cantilever beam has several advantages over other mechanical vibrators: it produces relatively low resonance frequencies and relatively high average strain for a given input force. However, a designer may not know this frequency a priori or the frequency might change over time. There are two possible ways to have a single design that is able to operate in a range of

frequencies: develop actuators to change the harvester's resonance frequency or develop designs for scavengers with wider bandwidths. Changing the resonant frequency by moving the mass will not possible. The paper has also shown that the tapered cantilever is more strain productive than simple rectangular one.

3. PROPOSED ENERGY HARVESTING METHODOLOGY

According to the table of energy harvesting productivity methods introduced in Table 2, piezoelectric based methods rank second among the different methods after solar cells. But as far as availability is concerned, it is the much accessible than sun light. Thus, because of accessibility and high productivity, vibration and piezoelectric-based energy harvesting was preferred and utilized. First a mathematical model was developed for PZT.

3.1 PZT Electromechanical Model

A vibrating piezoelectric device differs from a typical electrical power source since its internal impedance is capacitive rather than inductive in nature, and therefore it may be driven by a variable amplitude and frequency vibration. A simple schematic circuitry for PZT is depicted in Figure 2 in which the current source I_p is sinusoidal source with the frequency of ambient vibration
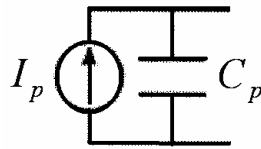

Figure 2. Schematic circuitry for PZT

The mathematical equations for a piezoelectric material are given by [13]

$$\delta = \frac{\sigma}{Y} + dE \tag{1}$$

$$D = \varepsilon E + d\sigma \tag{2}$$

where δ is mechanical strain , σ is mechanical stress, Y is Young's modulus, d is the piezoelectric strain coefficient, E is the electrical field, D is charge density, and ε is the dielectric constant of the piezoelectric material. Equations (1) and (2) can be transformed into more convenient form [9] as

$$F_P = K_{PE}u + \alpha V \tag{3}$$

$$I = \alpha \dot{u} - C_P \dot{V} \tag{4}$$

where F_P is mechanical force induced in the PZT, K_{PE} is the PZT equivalent spring constant, u is PZT displacement, I is the PZT output current, C_P is the PZT capacitance, and V is the PZT terminal voltage.

The geometric terms for bimorph mounted as a cantilever will be discussed next. The piezoelectric bender is a composite beam so an effective moment of inertia and elastic modulus are used. The effective moment of inertia is given by the equation below

$$I = 2[\frac{wt_c^3}{12} + wt_c b^2] + \eta_s wt_{sh}^3 \tag{5}$$

where w is the width of the beam, t_c is the thickness of an individual piezo, b is the distance from the center of the shim to the center of the piezo layers, t_{sh} is the thickness of the shim and η_s is the ratio of the piezo material elastic constant to that of the center of the shim (Beer and Johnston 1992). Instead of the force and displacement it is best to use stress and strain as the state equations for the system as the piezoelectric system deal directly with stress and strain. Two geometric constants are to be defined where the first relates vertical force to average stress and the second relates tip deflection of the beam to average strain in the piezo. The piezoelectric bender is shown in Figure 3. The average stress for the piezo material is defined as

$$\sigma = \frac{1}{l_e} \int \frac{M(x)b}{I dx}$$ (6)

where σ is stress, x is the distance from the base of the beam and M(x) is the moment in the beam as a function of x. The moment M(x) is defined as

$$M(x) = m(\ddot{y} + \ddot{z})(l_b + 0.5l_m - x)$$ (7)

where l_m is the length of the mass, $m(\ddot{y} + \ddot{z})$ is the input vibration in terms of acceleration and z is the vertical displacement of the beam.
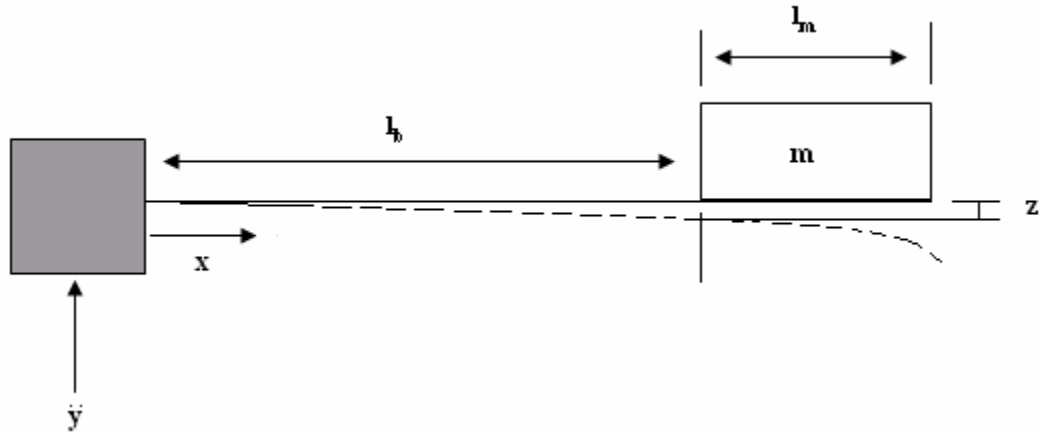

Figure 3. Schematic of piezoelectric bender

Substituting (7) in (6) we get

$$\sigma = m(\ddot{y} + \ddot{z})b\frac{(2l_b + l_m - l_e)}{2I}$$ (8)

The vertical force in the equation (8) is simply $m(\ddot{y} + \ddot{z})$. Therefore b^{**} is defined as shown below

$$b^{**} = \frac{2I}{b(2l_b + l_m - l_e)}$$ (9)

where b^{**} relates vertical force to stress (σ) and $\sigma = m(\ddot{y}+\ddot{z})/b^{**}$. To derive the second

geometric constant we consider the Euler beam equation which is given by

$$\frac{d^2 z}{dx^2} = \frac{M(x)}{Y_c I} \tag{10}$$

Substituting (7) in (10) we get

$$\frac{d^2 z}{dx^2} = \frac{1}{Y_c I} m(\ddot{y}+\ddot{z})(l_b + 0.5l_m - x) \tag{11}$$

Integrating the above expression for the deflection term toget

$$z = \frac{m(\ddot{y}+\ddot{z})}{2Y_c I}[(l_b + 0.5l_m)\frac{x^2}{2} - \frac{x^3}{6}]$$

At the point where the beam meets the mass ($x = l_b$) then z becomes

$$z = \frac{m(\ddot{y}+\ddot{z})}{2Y_c I}(2/3l_b + 0.5l_m)l_b^2 \tag{12}$$

By viewing strain as stress over elastic constant ($\delta = \sigma/Y$), stress can be written as (8)

from which strain becomes

$$\delta = \frac{m(\ddot{y}+\ddot{z})b}{2Y_c I}(2l_b + l_m - l_e)$$

Rearranging the above equation yields

$$m(\ddot{y}+\ddot{z}) = \frac{2Y_c I}{(2l_b + l_m - l_e)b} \tag{13}$$

Substituting (13) in (12) yields

$$z = \delta\frac{l_b^2}{3b}(\frac{(2l_b + 1.5l_m)}{(2l_b + l_m - l_e)}) \tag{14}$$

b^* relates strain to vertical displacement and is defined

$$b^* = \frac{3b}{l_b^2} \frac{(2l_b + l_m - l_e)}{(2l_b + 1.5l_m)} \tag{15}$$

3.2 Analytical Model for Piezo Electric Generators

In order to relate the amount of produced energy in the piezoelectric material to the ambient vibration, one needs an electromechanical model of a vibrating PZT. A simple structure is illustrated in Figure 4.

- The figure below shows the circuit model of the piezo electric generator.

- The across variable (variable across an element) and through variable (variable acting through an element) on the electrical side is voltage (V) and current (i), respectively

- The across and through variable on the mechanical side is stress (σ) and strain (δ).

- Mass attached is represented by an inductor and damper and it is shown as a resistor.

- Stiffness term is shown as capacitor and C_p is capacitor of bimorph

- The vibration input is shown as a stress generator (σ_{in}) which comes from the input acceleration ($\tilde{y}$)
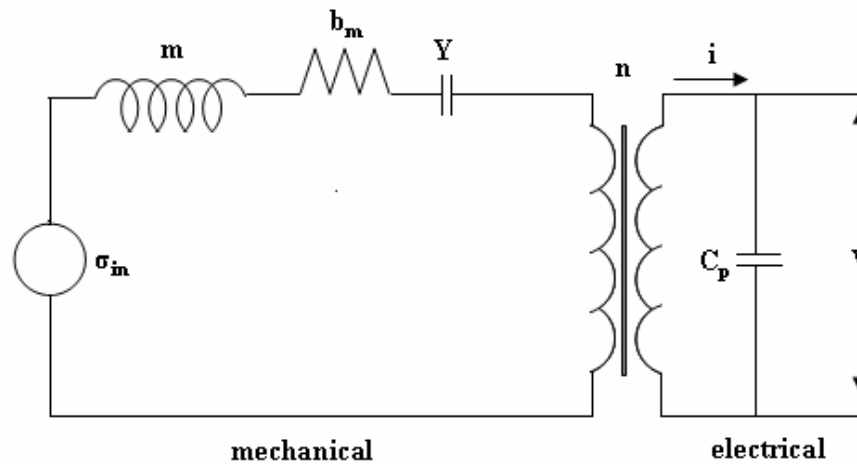

Figure 4. Circuit representation of piezoelectric bimorph

Equation (8) presents the stress resulting from both the input element σ_{in} and the inertial element *m*. The stress across the inductor represented as *m* is the stress developed as result of the mass flexing the beam. The relationship between σ_{in} and *m* is given in the below equations

$$\text{Input Stress } \sigma_{in} = (m/b^{**})y^{**} \tag{16}$$

$$\text{Stress across m } \sigma_{m} = (m/b^{**})\ddot{z} \tag{17}$$

Substituting strain for displacement in (17) and using the relationship from equations (14), (15) gives us the stress/strain relationship for the inductor

$$\text{Stress across m is } \sigma_{m} = (m/b^{*}b^{**})\delta^{**} \tag{18}$$

The damping coefficient b_m relates stress to tip displacement z. The stress strain relationship for the damping element b_m and the stiffness element is given as below

$$\text{Stress across damping element } \sigma_{bm} = (b_m/b^{*})\delta^{*} \tag{19}$$

$$\text{Stress across capacitor } \sigma_{Y} = Y_c\delta \tag{20}$$

where b* and b** is constant defined as in equation (15), (9)

The relationship between stress (σ), electric field (E), electrical displacement (D) and strain (δ) is given by

$$\delta = (\sigma/Y) + dE$$

$$D = \varepsilon E + d\sigma$$

For the transformer,

$$\sigma_t = -dY_cE \tag{21}$$

$$D_t = -dY_c\delta \tag{22}$$

Charge *q* and voltage *V* is given by

$$q = l_ewD \tag{23}$$

$$V = 2Et_c \tag{24}$$

where l_e is the electrode length, w is the width of the beam, D is the electrical displacement and t_c is the thickness of piezo which implies

$$\sigma_t = (-adY_c/2t_c)V \tag{25}$$

When we apply KVL to the circuit

$$\sigma_{in} = \sigma_m + \sigma_{bm} + \sigma_t + \sigma_Y \tag{26}$$

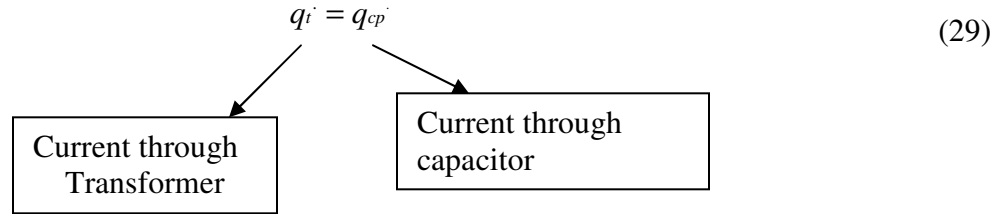$$(m/b^{**})y^{**} = (m/b^*b^{**})\ddot{\delta} + (b_m/b^*)\dot{\delta} - (adY_c/2t_c)V + Y_c\delta$$

$$(m/b^*b^{**})\ddot{\delta} = (m/b^{**})\ddot{y} - (b_m/b^*)\dot{\delta} + (adY_c/2t_c)V - Y_c\delta$$

$$\ddot{\delta} = b^*\ddot{y} - (b^{**}b_m/m)\dot{\delta} + (b^*b^{**}/m)(adY_c/2t_c)V - (Yb^*b^{**}/m)\delta \tag{27}$$

And here spring constant is taken as $K_{sp} = Yb^*b^{**}$ which implies

$$\ddot{\delta} = -(K_{sp}/m)\delta - (b_mb^{**}/m)\dot{\delta} + (K_{sp}da/2mt_c)V + b^*\ddot{y} \tag{28}$$

Applying KCL to the electrical side

$$\dot{q}_t = \dot{q}_{cp} \tag{29}$$

$$
\begin{aligned}
C_p &= (a^2\varepsilon\omega l_e/2t_c) \\
Q &= CV = (a^2\varepsilon\omega l_e/2t_c)V \\
I &= \frac{dQ}{dt} = \dot{q}_{cp} = (a^2\varepsilon\omega l_e/2t_c)\dot{V} \\
\dot{q}_t &= -dY_c al_e\omega\dot{\delta} \\
\dot{q}_t &= \dot{q}_{cp} \\
-dY_c al_e\omega\dot{\delta} &= (a^2\varepsilon\omega l_e/2t_c)\dot{V} \\
V &= -(2dY_c t_c/a\varepsilon)\dot{\delta}
\end{aligned}
\tag{30}
$$

Equations (1) and (2) constitute the dynamic model of the system which can be written in state space form as shown below

$$
\begin{bmatrix} \dot{\delta} \\ \ddot{\delta} \\ \dot{V} \end{bmatrix} = \begin{bmatrix} 0 & 1 & 0 \\ -\dfrac{K_{sp}}{M} & -\dfrac{b_m b^{**}}{M} & \dfrac{K_{SP}da}{2Mt_c} \\ 0 & \dfrac{-2dYt_c}{a\varepsilon} & 0 \end{bmatrix} \begin{bmatrix} \delta \\ \dot{\delta} \\ V \end{bmatrix} + \begin{bmatrix} 0 \\ b^* \\ 0 \end{bmatrix} \ddot{y}
$$

(31)

3.3 Beam Shaping

The above relations were developed for a rectangular beam. It is shown that in [19] that the tapered cantilever beam is more strain productive than simple rectangular beam as shown in the Figure 5. From this figure, it can be observed that the strain curves are different with the shape of the beam.
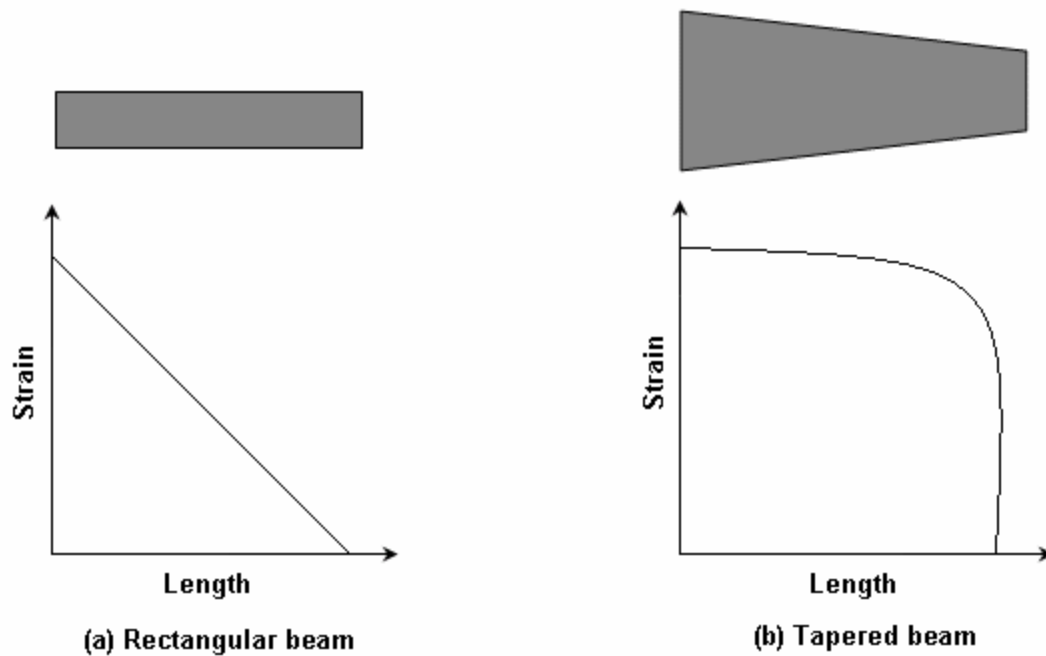

Figure 5. Strain in different beam geometries

Tapered beams are more productive and can provide more than 2 times of energy per unit volume of PZT material compared to rectangular beams for a given displacement since

the average strain is much higher in the former case. Next we derive the mathematical relations for the tapered beam and the tapered beam is shown in Figure 6.
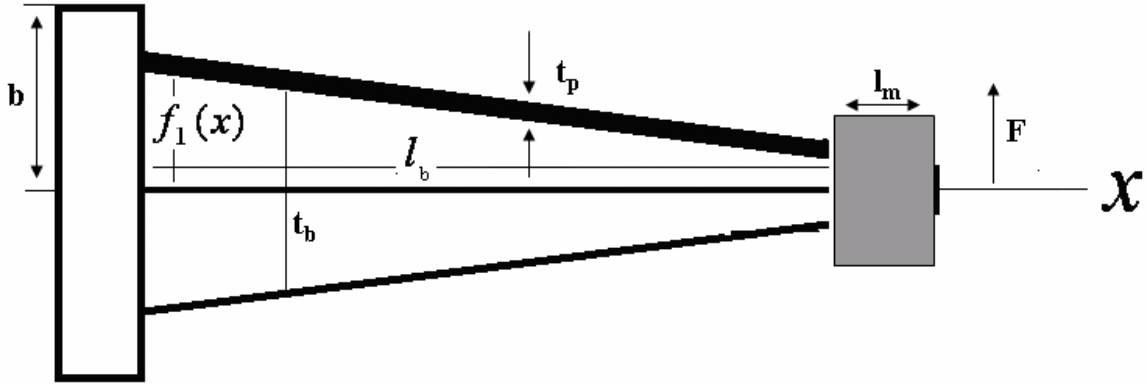

Figure 6. Tapered beam

On a tapered beam shown in Figure 6, the beam thickness is modeled by $f_1(x)$. So by adding a uniform PZT on the top of the beam the overall thickness is given by

$$f_2(x) = f_1(x) + \frac{t_p}{2} \tag{32}$$

where $f_2(x)$ is the distance from the center of the shim to the center of the piezo layers and $f_1(x)$ is the thickness of the shim. In the case of the tapered beam the geometric constants b^* and b^{**} will be different from the rectangular beam and these constants are updated in equation (31). The effective moment of inertia in this case is given as

$$
\begin{aligned}
I(x) &= 2(\frac{wt_p^3}{12} + wt_p f_2^2(x) + \frac{2\eta w f_1^3(x)}{3} \\
&= a_1 + a_2 f_2^2(x) + a_3 f_1^3(x)
\end{aligned} \tag{33}
$$

In this case also we define two geometric constants where the first relates vertical force to average stress and the second relates tip deflection of the beam to average strain in the piezo. The Moment M(x) is given as

$$\frac{M}{YI} = \frac{F}{YI(x)}(l_b + l_m/2 - x) \tag{34}$$

where Y is the young's modulus, I is the moment of inertia and F is the force on the beam.

The expression for the average stress in the piezo is given as

$$\sigma_{ave} = \frac{1}{l_b}\int_0^{l_p} \frac{Mf_2(x)}{I}dx$$

$$= \frac{F}{l_b}\int_0^{l_p} \frac{(l_b + 0.5l_m - x)f_2(x)}{a_1 + a_2 f_2^2(x) + a_3 f_1^3(x)}dx \tag{35}$$

The geometric constant b^{**} which relates vertical force to average stress is given as

$$b^{**} = \frac{F}{\sigma_{ave}} = \frac{l_b}{\int_0^{l_b} \frac{(l_b + 0.5l_m - x)f_2(x)}{(a_1 + a_2 f_2^2(x) + a_3 f_1^3(x))}dx} \tag{36}$$

We know that strain is stress over elastic constant ($\delta = \sigma/Y$) and stress can be written

as in equation (8) from which strain becomes

$$\delta_{ave} = \frac{F}{Yl_b}\int_0^{l_p} \frac{(l_b + 0.5l_m - x)f_2(x)}{a_1 + a_2 f_2^2(x) + a_3 f_1^3(x)}dx \tag{37}$$

The deflection term z mentioned in equation (12) is defined as

$$z = -\int_{x=0}^{l_b} \frac{M(x)}{EI(x)}xdx$$

$$= \frac{F}{E}\int_0^{l_b} \frac{(l_b + 0.5l_m - x)(l_b - x)}{a_1 + a_2 f_2^2(x) + a_3 f_1^3(x)}dx \tag{38}$$

The second geometric constant which relates the deflection of the beam to the average

strain in the piezo is given as

$$b^* = \frac{\delta}{z}$$

$$= \frac{\displaystyle\int_0^{l_p} \frac{(l_b + 0.5l_m - x)f_2(x)}{(a_1 + a_2 f_2^2(x) + a_3 f_1^3(x))} dx}{\displaystyle\int_0^{l_p} \frac{(l_b + 0.5l_m - x)(l_b - x)}{a_1 + a_2 f_2^2(x) + a_3 f_1^3(x)} dx} \tag{39}$$

These constants in equation (36) and (39) are substituted in equation (31) which represents the dynamic model of the system to get the output voltage.

4. EXPERIMENTAL SETUP

In order to validate the models presented in the previous section (Section 3) a PZT simulator has been developed which is able to predict the amount of AC and DC harvested power for an input frequency and acceleration which are given in applications. The experimental setup consists of the following hardware.

4.1 Piezoelectric Material

The piezoelectric material used in our setup is produced by Advanced Cerametric Inc. (ACI) which is a thin, flexible, strip of composite fiber with a laminate coating illustrated in Figure 7. The technology is called Piezoelectric Ceramic Fiber composite (PCFC) that can typically generate voltage outputs in the range of 40 Vp-p from minor vibration. A strong vibration with PCFCs can easily produce voltages in the range of 400 Vp-p. The material specifications are shown in Table 3.

Figure 7. PCFC material

Table 3. PCFC specifications

Specifications	Model PCFC-100
Substrate Material	Kapton or equivalent
Conductive Ink	Silver loaded epoxy
Fiber Type	PZT_5A
Dimensions	13.0cm X 1.0cm X 0.4cm
Average actual strain at $3KV_{pp}$ under 600 V dc bias (ppm)	1800
Operational voltage limits	-1500 to 2800
Vibration frequency range	Infinite
Relative permittivity K_{33}	495
Weight	1.8 grams
Dielectric constant at 1Khz	1725
K_{33}	72%
D_{33}	380(10e-12m/V)
Young's Modulus	6.6×10^{10} N/m^2

4.2 Shaker and Cantilever beam

The cantilever beam is made of steel wherein 4 pieces of PZTs are glued to the top and bottom. It is fixed within two clamps on the shaker rod at one end as depicted in Figure 8. The rectangular and tapered beam (not shown in figure) has dimensions of 16cm by 1.72cm by 0.13cm and a Young modulus of $21 \times 10^{10} \, N/m^2$.
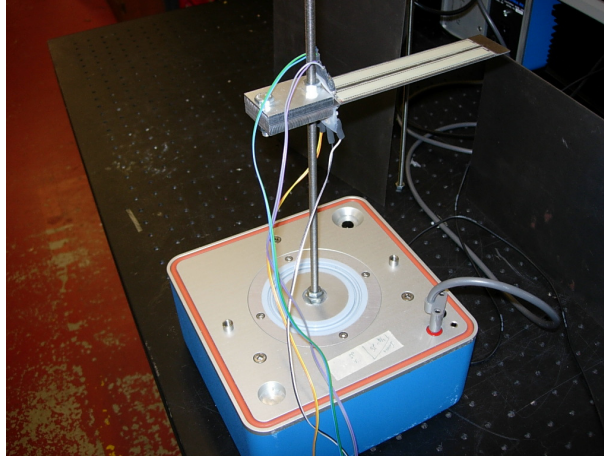
Figure 8. Shaker and rectangular beam

4.3 Rectifier and Power Converter

A DC/DC step-down converter can be employed to keep the DC voltage high and at the same time feed a low voltage sensor. The proposed step-down power converter which works under Discontinuous Conduction Mode (DCM) as depicted in Figure 9.
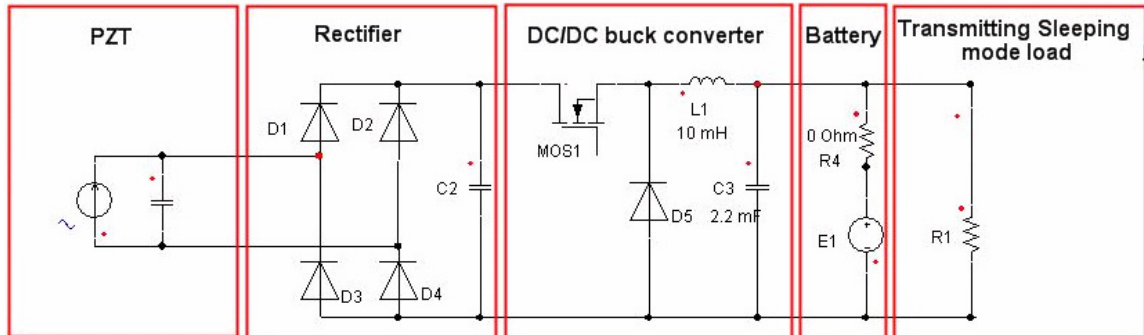

Figure 9. Step down buck converter connected between the rectifier and load

The entire circuitry now consists of a bridge rectifier with filter capacitor, a step-down DC/DC converter, UMR mote and a microcontroller board and gate commanding circuitry.

5. RESULTS

Based on the model presented in Section 3 a PZT simulator has been developed to predict the amount of AC and DC harvested power for an input frequency and acceleration which are given in the proposed application. The output voltage for the piezoelectric generator is obtained from (31) which is given below

$$
\begin{bmatrix} \dot{\delta} \\ \ddot{\delta} \\ \dot{V} \end{bmatrix} = \begin{bmatrix} 0 & 1 & 0 \\ -\dfrac{K_{sp}}{M} & -\dfrac{b_m b^{**}}{M} & \dfrac{K_{SP} da}{2Mt_c} \\ 0 & \dfrac{-2dYt_c}{a\varepsilon} & 0 \end{bmatrix} \begin{bmatrix} \delta \\ \dot{\delta} \\ V \end{bmatrix} + \begin{bmatrix} 0 \\ b^* \\ 0 \end{bmatrix} \ddot{y}
\tag{40}
$$

The term in which we are interested in the above equation is the voltage term V from which the power harvested is calculated.

5.1 AC Power

Considering a resistive load connected to the PZT as shown in Figure 10, the voltage on the piezoelectric element can be expressed in the frequency domain as a function of the displacement of free end tip of the cantilever beam u and angular frequency ω as follows
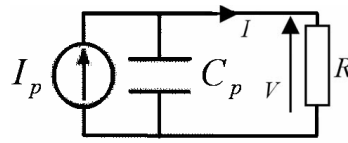

Figure 10. AC power

$$
\tilde{V} = \frac{\alpha R}{1 + jRC_p\omega} \tilde{u} j\omega
\tag{41}
$$

where α is the force factor, C_p is the capacitance of the piezo and using (41), the average harvested power can be expressed as a function of the displacement amplitude u_m as

$$P = \frac{\tilde{V}\tilde{V}^*}{2R} = \frac{R\alpha^2}{1+(RC_p\omega)^2} \frac{\omega^2 u_m^2}{2} \tag{42}$$

The power can be optimized using optimal load as

$$R_{opt} = \frac{1}{C_p\omega} \tag{43}$$

and

$$P_{max} = \frac{\alpha^2 \omega u_m^2}{4C_P} \tag{44}$$

5.2 DC Power

Remote sensors are basically fed by DC power and therefore ac power generated by the PZT should be rectified and filtered in order to have a fixed DC voltage. A rectifier followed by a filtering capacitance C_r and the load resistance R are connected to the piezoelectric element in Figure 11. The rectifier is assumed to be lossless and its voltage V_{cc} is assumed to be a constant. Under these conditions, the average current flowing through the filtering capacitance is zero during a half oscillating period.
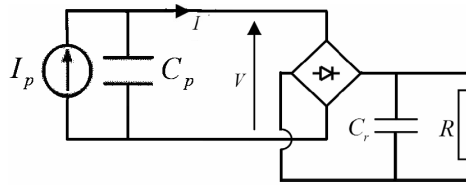

Figure 11. DC power

It is considered that the electric charge generated by the piezoelectric element during a particular semi period in which rectifier diodes are conducting is equal to the amount of charge consumed by the load as given by

$$\int_{t_1}^{t_2} Idt = \frac{V_{CC}}{R} \frac{T}{2} \tag{45}$$

Thus, the rectifier voltage V_{CC} and output power are given by

$$V_{CC} = \frac{R\alpha}{RC_P\omega + \dfrac{\pi}{2}}\omega u_m \tag{46}$$

and

$$P = \frac{V_{CC}^2}{R} = \frac{R\alpha^2}{(RC_P\omega + \dfrac{\pi}{2})^2}\omega^2 u_m^2 \tag{47}$$

The optimal load and maximum power in the case of dc power will then be

$$R_{opt} = \frac{\pi}{2C_P\omega} \tag{48}$$

and

$$P_{max} = \frac{\alpha^2\omega u_m^2}{2\pi C_P} \tag{49}$$

Consequently, the DC power is less than AC power by a factor of 2Π/4 theoretically. Also, comparing (41) and (46) for optimal DC load, one can conclude that maximum DC power is produced when the rectifier voltage is half of the maximum PZT AC voltage. The experimental results were calculated under the following conditions:

(a) Input vibration amplitude of 0.5mm

(b) Force factor α is given by $\alpha = 4.75\times10^{-4}VF/m$ and the displacement amplitude u_m is considered as $u_m = 2.5\times10^{-3}m$

(c) C_p = 2.5nF for individual PZT and the total capacitance of the beam (4 PZTs) is 10nF

(d) Dimensions of the beam are 16cmX1.72cmX0.13cm

(e) Mass M is 0.015g and t_c thickness of piezo is 0.4e-3

(f) Young's Modulus = $21\times10^{10}N/m^2$

 (g) a=2 as the piezoelectric layers are wired in parallel

(h) b^* and b^{**} are calculated by (15) and (9) for rectangular beam and (36), and (39) for the tapered beam.

A graph of DC harvested power versus frequency for rectangular beam and the tapered beam is shown in Figure 10. The natural frequency for the rectangular and tapered beams is given by 37Hz and 68Hz where maximum power is harvested. As expected, when the frequency moves away from the resonant frequency, the harvested power drops significantly. We can observe that the harvested power is higher in the case of the tapered beam as the strain is more evenly distributed over the beam. From Figure 10, it can be observed that the maximum harvested power for the rectangular beam is 3.5mW where as for the tapered beam the maximum harvested power is 20mW which is almost 5 times that of the rectangular beam.
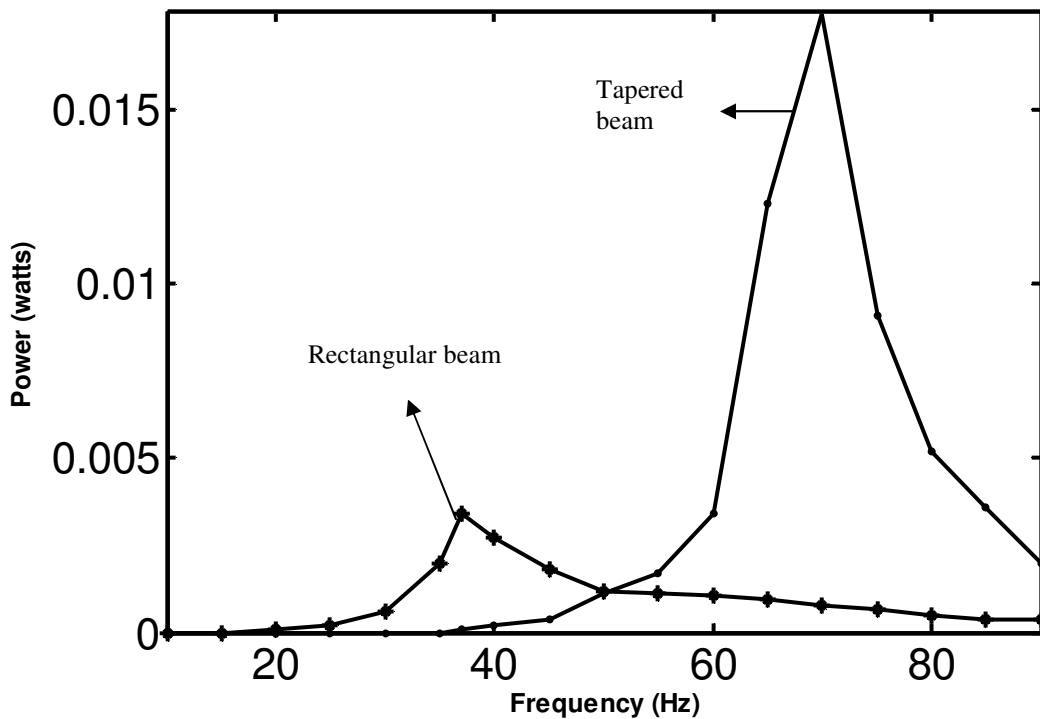
Figure 12. DC harvested power versus frequency

The reason why a tapered beam can harvest more power is because of more induced strain in the tapered beam which is evenly distributed throughout the beam. As the strain induced is higher, the geometric constants b^* and b^{**} given in (36) and (39) are higher and when substituted in (40) yields higher output voltage for the tapered beam as shown in Figure 11. The strain developed in rectangular beam is also shown in Figure11.
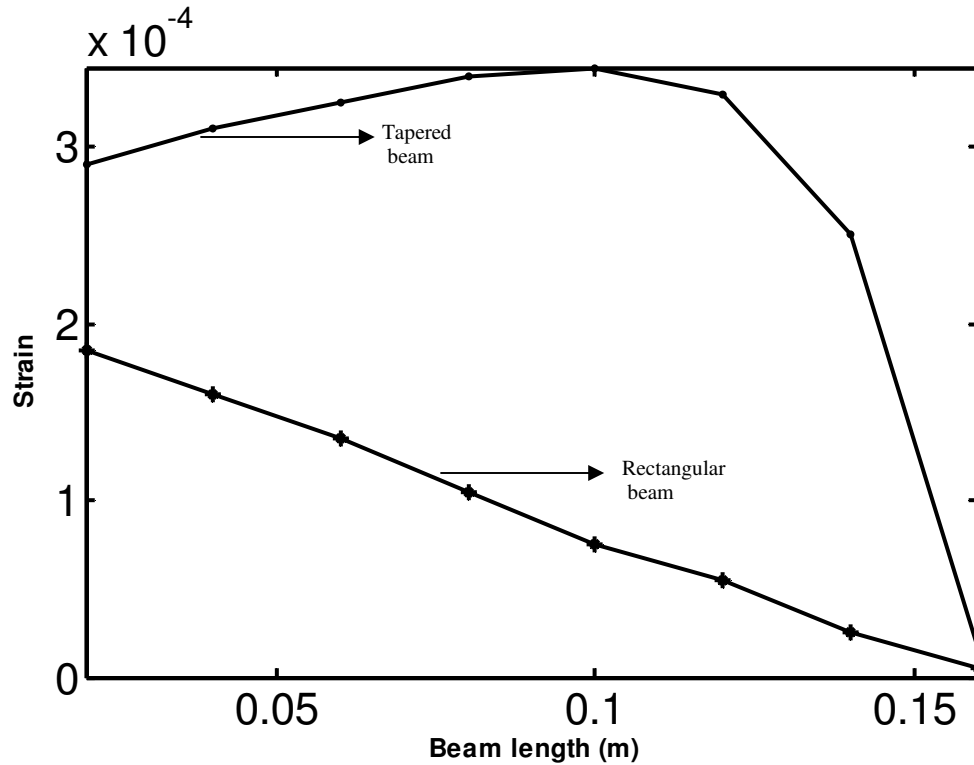

Figure 13. Comparison of strain

With the same volume of PZT and with the trapezoidal profile, the strain can be more evenly distributed such that the maximum strain is reached at every point in the piezo. So, the harvested power is higher in a tapered beam when compared with a rectangular beam.

5. CONCLUSIONS

The underlying concept of vibration based piezoelectric based energy harvesting is to extract energy from the environmental vibrations and provide it to the sensor node. In this work, the design of a new piezoelectric power generator using a tapered beam is discussed. The setup consists of a piezoelectric generator, AC/DC circuitry and a sensor node. Unlike previous studies, this work verifies the feasibility of powering such a sensor by placing the piezoelectric generator on a vibrating device. Our experimental results, al though not included in this work, reveal that vibration-based energy harvesting using piezoelectric material is capable of supporting low power sensors in an environment equipped with moving machinery where there is adequate amount of vibration.

Vibration based energy scavenging is a viable means of obtaining small quantities of energy necessary to power wireless sensor node. Current technology focuses on rectangular PZT structure which uses the piezo inefficiently. An effective beam design can potentially increase the amount of harvested energy which is made available by using more effective beam geometries. A tapered beam has been designed (trapezoidal) where the strain is distributed more evenly such that the maximum strain is reached at every point in the piezo. The harvested energy of a tapered beam is five times when compared with the power harvested using the rectangular beam. Also the high power sensors should have sleep mode in order to be fed by this energy scavenging method.

REFERENCES

[1] Crossbow Inc. http://www.xbow.com. MoteWorks Brochure. December 2006.

[2] Onsite Sycom Energy Corporation. Review of heat and power technologies. Office of Industrial Technologies, Office of Energy Efficiency and Renewable Energy, U.S Department of Energy, October 1999.

[3] Swarn S. Kalsi. The development status of superconducting rotating machines. IEEE Power Engineering Society Winter Meeting, pp 401-403, January 2002.

[4] Anantha P. Chandrakasan, Rajeevah Amirthrajah, James Goodman "Trends in low power digital signal processing," Proceedings of the IEEE International Symposium on Circuits and Systems, pp 30-35, 1998.

[5] Erick O. Torres, Gabriel A. Rincon-Mora, "Energy Harvesting Chips and Quest for Everlasting Life," IEEE Transactions on VLSI Systems, pp 39-45, June 2005.

[6] Moncef B. Tayahi, Bruce Johnson, "Piezoelectric Generator for Powering Remote Sensor Networks," IEEE International Conference on Performance, Computing and Communications, pp 383-386, April 2005.

[7] S. Roundy, B. Otis, Y.H. Chee, J.M. Rabaey, P. Wright, "A 1.9 GHz RF transceiver beacon using environmentally scavenged energy," International Symposium on Low Power Electronics and Design, pp 343-348, Seoul, Korea, August 2003

[8] C. Shearwood, R.B. Yates, "Development of an electromagnetic micro generator," Electronics Letters, IEEE Transactions on Power Electronics, vol 33, pp 103-108, 1997.

[9] S. Meninger, J.O. Mur Miranda, R. Amritharajah, A.P. Chandrakasan, J.H. Lang, "Vibration to electric energy conversion," IEEE Transactions on VLSI Systems, pp112-117, 2001.

[10] S. Roundy, P.K. Wright, K.S.J. Pister, "Micro electrostatic vibration to electricity converters," ASME IMECE, pp 176-181, New Orleans, Louisiana, November 2002.

[11] G.K. Ottman, H.F. Hofmann, G.A. Lesieuture, "Optimized piezoelectric energy harvesting circuit using step down converter in discontinuous conduction mode," IEEE Transactions on Power Electronics, vol 18, pp 696-703, 2003.

[12] S. Roundy, P.K. Wright, J. Rabaey, "A study of low level vibrations as a power source for wireless sensor nodes," Computer Communications, vol 26, pp 14-18, 2003.

[13] G. Despesse, Jager T, Chaillout J, Léger J, Basrour S, "Design and Fabrication of a New System For Vibration Energy Harvesting," Proceedings of the IEEE Ultrasonic Symposium, pp 946-949, 2005.

[14] V. Raghunathan, A. Kansal, and M. Srivastava, "Design Considerations for Solar Energy Harvesting Wireless Embedded Systems," Proceedings of the IEEE, pp 457-462, 2005.

[15] S.W. Arms, C.P. Townsend, D.L. Churchill, J.H. Galbreath, S.W. Mundell," Power Management for Energy Harvesting Wireless Sensors," Society of Photographic Instrumentation Engineers International Symposium on Smart Structures & Smart Materials, pp 78-84, San Diego, CA 2005.

[16] D.L. Churchill, M.J. Hamel, C.P. Townsend, S.W. Arms, MicroStrin Inc, Power point, 2003.

[17] T. J. Johnson and W. Clark," Works in Progress," IEEE Pervasive Computing, pp 70-71, 2005.

[18] S. Roundy, P.K. Wright, and J. Rabaey, Energy Scavenging for Wireless Sensor Networks with Special Focus on Vibrations, Kluwer Academic Press, 2003.

[19] S. Roundy, "Improving Power Output for Vibration based Energy Scavengers," Pervasive Computing, IEEE Computer Society, pp 87-93, 2005.

[20] E. P. James, M. J. Tudor, S. P. Beeby, N. R. Harris, P. Glynne Jones, J. N. Ross, N. M. White, "An investigation of self powered systems for conditioning monitoring applications," Sensors and Actuators A: Physical, vol 110, pp. 171-176, 2004.

VITA

Phani Kumar Gajjala was born in Suryapet, Andhra Pradesh, India on May 28, 1984. He completed his Bachelor of Technology degree in Electronics and Communication from Bapatla Engineering College in 2005. He joined University of Missouri-Rolla in Fall 2005 for a Master of Science program in Computer Engineering and received the degree in December 2007.